

# On the Negative Correlation of Stochastic Voltage Dependent Loads

Muhammad Adeen  
Transmission System Operator,  
EirGrid, plc, Ireland  
dr.muhammad.adeen@gmail.com

Federico Milano  
School of Electrical and Electronic Engineering  
University College Dublin, Ireland  
federico.milano@ucd.ie

**Abstract**—This paper discusses the effect of voltage dependency on stochastic loads. The study shows that the higher the exponent of the voltage in the load model, the higher the correlation of the active and reactive power consumption. Counterintuitively, this correlation is negative. As a consequence, the higher the exponent of the voltage, the less the impact of the noise on the dynamic behavior of the system. The paper provides a theoretical development that supports this conclusion as well as a comprehensive case study based on a well-known benchmark system.

**Index Terms**—Stochastic processes, probability distribution function, standard deviation, volatility, power system dynamic performance, voltage-dependent load.

## I. INTRODUCTION

### A. Motivation

The voltage dependence of loads has a key role in the stability analysis of power systems. Constant power loads tend to create more stability issues such as reducing the voltage stability margin [1], and worsening the effect of power unbalance and faults [2]–[5], than constant current and constant impedance ones. Recent studies on the stochastic nature of loads have shown that correlation plays a similar role than voltage dependence on the transient response of the system. That is, for loads with same probability distribution, mean and standard deviations, the higher the correlation, the higher the probability that the system becomes unstable [6], [7]. Previous studies, however, ignore the voltage dependency of the loads. The impact of load voltage dependency on the stochastic behavior of loads is the focus of this work.

### B. Literature Review

Modeling the load accurately based on the measurement data is an essential tool for power system dynamic and stability studies. For example, [1] and [5] provide comprehensive discussions on the impact of various load models on the power system voltage stability. Several studies have proposed various load models such as voltage dependent loads, composite loads [8], [9], exponential recovery loads [10], [11], dynamic loads [12], and ZIP loads [13] to name a few. A general overview

on load modeling and aggregation can be found in [14]. A literature extensive review on load models can be found in [15].

The references mentioned above model load consumption via traditional deterministic models that often fail to capture the randomness in loads in the time scale of power system dynamic. This leads to inaccurate estimation of the power system dynamic behavior. For this reason, this paper utilizes stochastic load models to study the dynamic of the power system. Stochastic load models are capable of capturing the uncertainty and volatility arising due to the non-deterministic nature of the load consumption.

Load power consumption with noise is the focus of this work. We are, in particular, interested in modeling the volatility of the power consumption, which can be represented through a Stationary Stochastic Process (SSP), which is defined in Appendix A, [16], [17]. A SSP is characterized by autocorrelation that defines the speed of the process, correlation, i.e., the similarity between the processes and Probability Density Function (PDF). The effect of volatility on the power system dynamic is modeled via Stochastic Differential-Algebraic Equations (SDAEs) [18].

In recent years, the impact of volatility introduced through load consumption has been studied in various works. For example, the effect of stochastic loads on the oscillatory modes of the power system was studied in [19]. The impact of autocorrelation of stochastic loads on the power system dynamic is discussed in [20]. References [6] and [7] demonstrate that the correlated stochastic loads worsen the power system dynamic. Reference [21] studies the impact of stochastic loads modeled with similar statistical properties but different PDFs on the statistical properties of the power system quantities. All the aforementioned studies analyze the behavior of stochastic loads and their effect on the power system dynamic performance but consider constant power load models, thus neglecting the effect of the voltage dependence of the power consumption.

### C. Contributions

This work provides a discussion on the impact of voltage dependence of stochastic load models on the power system dynamic response. We show, through analytical developments, that the variances and covariances of the active and reactive

---

This work is partly supported by Sustainable Energy Authority of Ireland (SEAI), by funding F. Milano under the project FRESLIPS, Grant No. RDD/00681.

load power consumption are a function of the voltage dependence of the loads. The effect is counterintuitive as the higher the voltage dependence, the least the correlation between active and reactive powers. The paper qualitatively and quantitatively illustrates the link between power correlation and voltage dependence. Load models are set up using real-world measurement data.

#### D. Organization

The remainder of the paper is organized as follows. Multi-dimensional SDAEs to model stochastic processes in power systems are introduced in Section II-A. The voltage dependent stochastic load model is described in Section II-B. Section III introduces load models with inclusion of correlated SSPs and studies the statistical properties of these models. The expressions for means, variances, and covariances of the load active and reactive power consumption, as well as bus voltage magnitudes are provided in Section IV. Section V presents a case study based on the WSCC 9-bus system where loads are modeled as voltage dependent stochastic loads, and evaluates the effect of voltage dependence of these loads on the dynamic performance of the system. Finally, Section VI draws conclusions.

## II. MODELING

### A. Stochastic Differential-Algebraic Equations

Multi-dimensional SDAEs that model stochastic processes in power system dynamic models are written as:

$$\dot{\mathbf{x}} = \mathbf{f}(\mathbf{x}, \mathbf{y}, \boldsymbol{\kappa}), \quad (1)$$

$$\mathbf{0} = \mathbf{g}(\mathbf{x}, \mathbf{y}, \boldsymbol{\kappa}), \quad (2)$$

$$\dot{\boldsymbol{\kappa}} = \mathbf{a}(\boldsymbol{\kappa}) + \mathbf{b}(\boldsymbol{\kappa}) \odot \mathbf{C}\boldsymbol{\xi}, \quad (3)$$

where  $\mathbf{f}$  and  $\mathbf{g}$  are the differential and algebraic equations, respectively;  $\mathbf{x} \in \mathbb{R}^n$  and  $\mathbf{y} \in \mathbb{R}^m$  are the vectors of state and algebraic variables, respectively.  $\boldsymbol{\kappa} \in \mathbb{R}^{n_\kappa}$  are correlated stochastic processes;  $\mathbf{a} \in \mathbb{R}^{n_\kappa}$  and  $\mathbf{b} : \mathbb{R}^{n_\kappa}$  are the *drift*, and *diffusion* terms, respectively. If the drift is a vector of linear functions, e.g.  $\mathbf{a}(\boldsymbol{\kappa}) = \boldsymbol{\alpha} \circ \boldsymbol{\kappa}$ , the elements of the vector  $\boldsymbol{\alpha}$  are called *autocorrelation coefficients*.  $\odot$  represents the element-by-element product of two vectors.  $\mathbf{C}$  is a lower-triangular matrix and satisfies:

$$\mathbf{R} = \mathbf{C}\mathbf{C}^T, \quad (4)$$

where  $\mathbf{R}$  is a semi-positive definite matrix such that its diagonal elements are 1 and off-diagonal elements define the correlation between the dependent processes. Finally,  $\boldsymbol{\xi} \in \mathbb{R}^{n_\xi}$  is a vector of  $n_\xi$ -dimensional independent *Gaussian white noise*, which is the formal representation of time derivative of the Wiener process.

Equations (3) are SDEs that can be formally integrated to obtain:

$$\boldsymbol{\kappa}(t) = \boldsymbol{\kappa}_0 + \int_{t_0}^t \mathbf{a}(\boldsymbol{\kappa}(s))ds + \int_{t_0}^t \mathbf{b}(\boldsymbol{\kappa}(s))d\mathbf{W}(s). \quad (5)$$

In (5), the integral of drift term is a deterministic integral and is represented traditionally as a Riemann-Stieltjes integral.

Several, integration schemes are available to solve this integral. Whereas, the integration of the diffusion term involves the Wiener process, which makes this integral non-deterministic. In power systems, the stochastic integral is usually integrated using Itô's calculus [22]. The interested reader can find the details and the challenges of the numerical integration of SDEs in [23] and [24]. Based on the recommendations given in these books, in this paper, the Euler-Maruyama method with sufficiently small time steps is utilized (see also [18]).

### B. Voltage Dependent Load Model

In the literature, voltage dependent stochastic loads are modeled by introducing stochastic processes into voltage dependent loads [16], [25], as follows:

$$\begin{aligned} p_L(t) &= (\kappa_p(t))(\tilde{v})^\gamma \\ q_L(t) &= (\kappa_q(t))(\tilde{v})^\gamma, \end{aligned} \quad (6)$$

where  $p_L(t)$  is the active power and  $q_L(t)$  is the reactive power of the load consumption;  $\kappa_p(t)$  and  $\kappa_q(t)$  are dependent SSPs defined as in (3) and  $\tilde{v}$  is:

$$\tilde{v} = v(t)/v_0, \quad (7)$$

where  $v(t)$  and  $v_0$  are the voltage magnitude at the load bus at time  $t$  and at the initialization of the simulation, i.e.,  $v_0 = v(0)$ , respectively. The exponent  $\gamma$  in (6) is responsible for defining the voltage dependence of the load. For example, to impose constant power loads  $\gamma$  takes a value of zero;  $\gamma = 1$  imposes constant current loads; and constant impedance loads are achieved at  $\gamma = 2$ . Note that voltage dependent loads are more general than ZIP loads, as these can be considered a second order Taylor expansion of equations (6). For this reason, in this work we consider only voltage dependent loads.

## III. DEPENDENT STATIONARY STOCHASTIC PROCESSES

This section aims at determining the statistical properties, i.e., means, variances, and covariances, of the SSPs in the load model in (6). Appendix A provides the definition of a SSP. The voltage dependent load model in (6) comprises of three dependent SSPs, i.e.,  $\kappa_p$ ,  $\kappa_q$  and  $\tilde{v}$ . It is shown in Appendix B that  $v$  is also a SSP if  $p_L$  and  $q_L$  are SSPs. To simplify the calculations for the statistical properties;  $\kappa_p$ ,  $\kappa_q$  and  $\tilde{v}$  are defined in terms of dependent SSPs using (3).

First, we introduce a SSP  $\kappa$  in (3) in its integral form as [26]:

$$\kappa(t) = \mu(\kappa) + e^{-\alpha_\kappa t}[\kappa_0 - \mu(\kappa)] + \int_0^t e^{-\alpha_\kappa(t-s)} b_\kappa dW_\kappa(s), \quad (8)$$

where  $\mu(\kappa)$  is the mean of  $\kappa(t)$ ;  $\kappa_0$  is the initial value of  $\kappa(t)$  at  $t = 0$ ; and  $\alpha_\kappa$  is the autocorrelation coefficient of  $\kappa(t)$ . For  $\kappa_0 = \mu(\kappa)$ , (8) becomes:

$$\kappa(t) = \mu(\kappa) + \int_0^t e^{-\alpha_\kappa(t-s)} b_\kappa dW_\kappa(s). \quad (9)$$

The dependent SSPs, i.e.,  $\kappa_p$ ,  $\kappa_q$  and  $\tilde{v}$ , can be written as:

$$\begin{bmatrix} \kappa_p \\ \kappa_q \\ \tilde{v} \end{bmatrix} = \begin{bmatrix} p_{L0} \\ q_{L0} \\ 1 \end{bmatrix} + \begin{bmatrix} \int_0^t e^{-\alpha_p(t-s)} b_p \\ \int_0^t e^{-\alpha_q(t-s)} b_q \\ \frac{1}{v_0} \int_0^t e^{-\alpha_v(t-s)} b_v \end{bmatrix} \odot \mathbf{C} \begin{bmatrix} dW_p(s) \\ dW_q(s) \\ dW_v(s) \end{bmatrix}, \quad (10)$$

where  $\mu(\kappa_p) = \kappa_p(t_0) = p_{L0}$ ;  $\mu(\kappa_q) = \kappa_q(t_0) = q_{L0}$ ;  $\mu(v) = v_0$ ; and  $\mathbf{C}$  has the same meaning as in (3).

In (10),  $v$  is defined as a process dependent on the two SSPs of  $\kappa_p$ , and  $\kappa_q$ . The exact mathematical formulation is given in Appendix B. For the sake of simplicity but without loss of generality, we assume that the processes  $\kappa_p$  and  $\kappa_q$  are normally distributed.<sup>1</sup> This makes  $v$  in (32) and consequently  $\tilde{v}$  in (10) normally distributed as well. In case of normal distribution, the diffusion function  $b$  in (10) becomes a constant and can be written as  $b = \sqrt{2\alpha}\sigma$ , where  $\sigma$  is the standard deviation of the normally distributed process.

The means and variances of  $\kappa_p$ ,  $\kappa_q$  and  $\tilde{v}$  in (10) are:

$$\begin{aligned} E[\kappa_p] &= p_{L0}, & E[\kappa_q] &= q_{L0}, & E[\tilde{v}] &= 1, \\ V[\kappa_p] &= \frac{b_p^2}{2\alpha_p}, & V[\kappa_q] &= \frac{b_q^2}{2\alpha_q}, & V[\tilde{v}] &= \frac{1}{v_0^2}\sigma^2(v), \end{aligned} \quad (11)$$

where  $E[\cdot]$  is the expectation operator;  $V[\cdot]$  is the variance operator; and  $\sigma^2(v) = b_v^2/2\alpha_v$ . Since, term  $\tilde{v}^2$  appears in constant impedance loads. The mean and variance of  $\tilde{v}^2$  are given as:

$$E[\tilde{v}^2] = E[\tilde{v}] = 1, \quad V[\tilde{v}^2] = 4V[\tilde{v}]. \quad (12)$$

The covariances of  $\kappa_p$ ,  $\kappa_q$ ,  $v$  and  $\tilde{v}^2$  are defined as:

$$\begin{aligned} C(\kappa_p, \kappa_q) &= 2 \frac{\sqrt{\alpha_p \alpha_q}}{\alpha_p + \alpha_q} \sigma(\kappa_p) \sigma(\kappa_q) r_{pq}, \\ C(\kappa_p, \tilde{v}) &= 2 \frac{\sqrt{\alpha_p \alpha_v}}{v_0^2(\alpha_p + \alpha_v)} \sigma(\kappa_p) \sigma(v) r_{p\tilde{v}}, \\ C(\kappa_q, \tilde{v}) &= 2 \frac{\sqrt{\alpha_q \alpha_v}}{v_0^2(\alpha_q + \alpha_v)} \sigma(\kappa_q) \sigma(v) r_{q\tilde{v}}, \\ C(\kappa_p, \tilde{v}^2) &= 2C(\kappa_p, \tilde{v}), \\ C(\kappa_q, \tilde{v}^2) &= 2C(\kappa_q, \tilde{v}), \end{aligned} \quad (13)$$

where  $C$  is the covariance operator;  $r_{pq}$  is the correlation between  $\kappa_p$  and  $\kappa_q$ ;  $r_{p\tilde{v}}$  is the correlation between  $\kappa_p$  and  $\tilde{v}$ ; and  $r_{q\tilde{v}}$  is the correlation between  $\kappa_q$  and  $\tilde{v}$ .

Note that in (13), the covariances  $C(X, Y)$  are the product of the individual variances ( $\sigma(X)$  and  $\sigma(Y)$ ) with the correlation ( $r_{X,Y}$ ) between the processes  $X$  and  $Y$  and some additional terms. It is known that  $r \in [-1, 1]$  and  $\sigma(X) < E[X]$ . The product of the terms in (13), ensures that:

$$E[\cdot] \gg C(\cdot, \cdot), \quad (14)$$

<sup>1</sup>The theory of stochastic differential equations utilizes, as building block, Wiener processes, which are normally distributed. Any other stochastic process can be built based on this building block. Of course, the maths becomes more involved as the drift and/or diffusion term can be nonlinear in general, but since all processes are ultimately built starting from normally distributed Wiener processes, there is no loss of generality considering that the load parameters are normally distributed.

As an example of (14), it can be said that  $E[\kappa_p] \gg C(\kappa_p, \tilde{v}^2) > C(\kappa_p, \tilde{v})$ , i.e., the mean is always greater than the variance and covariance.

#### IV. MOMENTS OF $p$ , $q$ AND $v$

In this section, we provide the definitions of the moments, i.e., mean, variance and covariance of the load consumption, i.e.,  $p_L$  and  $q_L$ , and voltage magnitude  $v$ . Note that  $p$  and  $q$  are products of dependent SSPs, i.e.,  $\kappa_p$  and  $\kappa_q$  with  $\tilde{v}$  or  $\tilde{v}^2$ , respectively. We first define the mean of  $p_L$  and  $q_L$  for all the three values of  $\gamma$  in (6).

The mean of the product of two dependent random variables  $X$  and  $Y$  is given as:

$$E[XY] = E[X]E[Y] + C(X, Y), \quad (15)$$

Using the results from (12) and (14), the mean of  $p$  and  $q$  for all the values of  $\gamma$  are:

$$\begin{aligned} E_p[p_L] &= E_i[p_L] = E_z[p_L] = p_{L0}, \\ E_p[q_L] &= E_i[q_L] = E_z[q_L] = q_{L0}, \end{aligned} \quad (16)$$

where the subscript  $p$  is for constant power,  $i$  is for constant current, and  $z$  is for constant impedance loads. Note that the means of  $p_L$  and  $q_L$  remain unchanged despite the degree of the dependence of the loads on the voltage.

Next, the definitions for variances of  $p_L$  and  $q_L$  are provided for all the cases of voltage dependence of loads. For this reason, the variance of the product of two dependent random variables  $X$  and  $Y$  are written in terms of their individual moments as [27]:

$$\begin{aligned} V(XY) &= (E[X])^2 V(Y) + (E[Y])^2 V(X) + E[(\Delta X)^2 (\Delta Y)^2] \\ &\quad + 2E[X]E[(\Delta X)(\Delta Y)^2] + 2E[Y]E[(\Delta X)(\Delta Y)^2] \\ &\quad + 2E[X]E[Y]C(X, Y) - (C(X, Y))^2, \end{aligned} \quad (17)$$

where  $\Delta X = X - E[X]$ .

Substituting (11), (12) and (13) into (17), the variances of  $p$  and  $q$  are given as:

$$\begin{aligned} V_p[p_L] &= [\sigma(\kappa_p)]^2, \\ V_p[q_L] &= [\sigma(\kappa_q)]^2, \end{aligned} \quad (18)$$

$$\begin{aligned} V_i[p_L] &= [\sigma(\kappa_p)]^2 + [p_{L0}\sigma(\tilde{v})]^2 \\ &\quad + 2p_{L0}C(\kappa_p, \tilde{v}) - [C(\kappa_p, \tilde{v})]^2, \\ V_i[q_L] &= [\sigma(\kappa_q)]^2 + [q_{L0}\sigma(\tilde{v})]^2 \\ &\quad + 2q_{L0}C(\kappa_q, \tilde{v}) - [C(\kappa_q, \tilde{v})]^2, \end{aligned} \quad (19)$$

$$\begin{aligned} V_z[p_L] &= [\sigma(\kappa_p)]^2 + 4[p_{L0}\sigma(\tilde{v})]^2 \\ &\quad + 4p_{L0}C(\kappa_p, \tilde{v}) - 4[C(\kappa_p, \tilde{v})]^2, \\ V_z[q_L] &= [\sigma(\kappa_q)]^2 + 4[q_{L0}\sigma(\tilde{v})]^2 \\ &\quad + 4q_{L0}C(\kappa_q, \tilde{v}) - 4[C(\kappa_q, \tilde{v})]^2. \end{aligned} \quad (20)$$

Note that the higher order moments, i.e., moments above 2nd order disappear due to the properties of the Wiener process. Note also that the expressions of the variances  $V_i[\cdot]$  and  $V_z[\cdot]$  show extra terms as compared to the variances  $V_p[\cdot]$ . On the one hand, the last term on the r.h.s of (19) and (20) is the

square of the covariance which is a very small number as compared to other three terms. This term has negligible effect on the variances. On the other hand, the third term on the r.h.s of (19) and (20) is significant enough to make a difference in the variances because it is a product of the covariance with the mean, which is a larger number.

The relationship between the variances of loads depends on the sign of the covariance of  $v$  vs  $\kappa_p$  and  $\kappa_q$ . Or, equivalently, the dependence of  $v$  on  $\kappa_p$  and  $\kappa_q$ . This can be written as:

$$\begin{aligned} V_p[\cdot] > V_i[\cdot] > V_z[\cdot] & \text{ if } -\infty < C(\kappa, \tilde{v}) < 0, \\ V_p[\cdot] < V_i[\cdot] < V_z[\cdot] & \text{ if } 0 < C(\kappa, \tilde{v}) < \infty. \end{aligned} \quad (21)$$

This is shown in Fig. 1 by illustrating the error on the variances, i.e.,  $V_p[\cdot]$  vs  $V_i[\cdot]$  and  $V_z[\cdot]$ . The error is calculated as:

$$\text{error \%} = \frac{\text{value} - \text{base}}{\text{base}} \times 100. \quad (22)$$

Next, we provide the definitions for the covariances of  $p_L$  and  $q_L$ . The covariance of the product of random dependent variables  $X$ ,  $Y$  and  $Z$  is written as [28]:

$$\begin{aligned} C(XY, ZY) &= E[Y]E[Y]C(X, Z) + E[Y]E[Z]C(X, Y) \\ &+ E[X]E[Y]C(Y, Z) + E[X]E[Y]C(Y, Y). \end{aligned} \quad (23)$$

Substituting the definitions of all the moments of  $\kappa_p$ ,  $\kappa_q$  and  $\tilde{v}$  into (23), the covariances of  $p$  and  $q$  for all the cases of voltage dependence are given as:

$$C_p(p_L, q_L) = 2 \frac{\sqrt{\alpha_p \alpha_q}}{\alpha_p + \alpha_q} \sigma(\kappa_p) \sigma(\kappa_q) r_{pq}, \quad (24)$$

$$\begin{aligned} C_i(p_L, q_L) &= C_p(p_L, q_L) + p_{L0} q_{L0} V[\tilde{v}] \\ &+ p_{L0} C(\kappa_q, \tilde{v}) + q_{L0} C(\kappa_p, \tilde{v}), \end{aligned} \quad (25)$$

$$\begin{aligned} C_z(p_L, q_L) &= C_p(p_L, q_L) + 2p_{L0} q_{L0} V[\tilde{v}] \\ &+ 2p_{L0} C(\kappa_q, \tilde{v}) + 2q_{L0} C(\kappa_p, \tilde{v}). \end{aligned} \quad (26)$$

Similar to variances, covariances of  $p_L$  and  $q_L$  involve extra terms for constant current and constant impedance loads. The last two terms on the r.h.s. of (25) and (26) can either be positive or negative simultaneously. For both cases of positive or negative dependence of  $v$  on  $p_L$  and  $q_L$ , one has:

$$\begin{aligned} C_p[\cdot] > C_i[\cdot] > C_z[\cdot] & \text{ if } -\infty < C(\kappa, \tilde{v}) < 0, \\ C_p[\cdot] < C_i[\cdot] < C_z[\cdot] & \text{ if } 0 < C(\kappa, \tilde{v}) < \infty. \end{aligned} \quad (27)$$

This is illustrated in Fig. 2, where the error on covariances, i.e.,  $C_p[\cdot]$  vs  $C_i[\cdot]$  and  $C_z[\cdot]$  is shown.

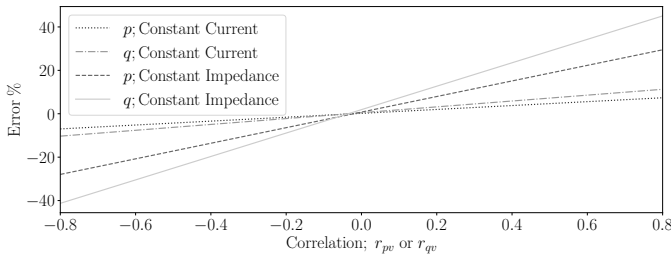


Fig. 1: Percent error on variances, calculated with (22) using  $V_p[\cdot]$  as base.

The definitions of variances in (18), (19) and (20) and covariances in (24), (25) and (26) indicate that the variances and covariances of  $p_L$  and  $q_L$  depend on the sign of the covariances of  $\kappa_p$  and  $\kappa_q$  with the bus voltage. This is confirmed by the plots shown in Figs. 1 and 2.

In stationary conditions, the mean and variance of  $v$  given in (32) — see the Appendix — are:

$$E[v] = v(p_{L0}, q_{L0}) = v_0, \quad (28)$$

$$V[v] = a_p^2 V[p_L] + a_q^2 V[q_L] + 2a_p a_q C(p_L, q_L). \quad (29)$$

where  $a_p$  and  $a_q$  are the partial derivatives of  $v$  with respect to  $\kappa_p$  and  $\kappa_q$ , respectively. The autocorrelation of  $v$  is:

$$R_v(\tau) = a_p^2 e^{-\alpha_p \tau} + a_q^2 e^{-\alpha_q \tau}. \quad (30)$$

As mean, variance and autocovariance of  $v$  do not depend on time,  $v$  satisfies the conditions outlined in (31) and is proven to be wide-sense stationary.

The mean of  $v$  only depends on the means of  $p_L$  and  $q_L$ , as long as  $E[p_L] = p_{L0}$  and  $E[q_L] = q_{L0}$ . The variance of  $v$  is the weighted sum of the variances and covariances of  $p_L$  and  $q_L$ . Similarly, the autocorrelation function of  $v$  is the weighted sum of the autocorrelation functions of  $p_L$  and  $q_L$ . These results indicate that the variance of  $v$  changes with the modification of voltage dependence of  $\kappa_p$  and  $\kappa_q$  because it modifies the variances of  $p_L$  and  $q_L$ .

## V. CASE STUDY

This section studies the effect of voltage dependence of the stochastic loads on the power system dynamic. With this aim, we use the WSCC test system, which includes 9 buses, 9 lines/transformers, 3 load devices and 3 synchronous machines that are equipped with turbine governors, an automatic generation control and automatic voltage regulators to avoid any unrealistic instabilities. In the simulations, the deterministic part of the SDAEs is integrated with trapezoidal method with a time step  $\Delta t = 0.01$  s and the stochastic integral is interpreted as an Itô's integral and integrated using the Euler-Maruyama integration scheme with a step size  $h = 0.01$  s. All simulations were solved using the software tool Dome [29].

Load consumption is modeled via voltage dependent stochastic load model using (6). The processes  $\kappa_p$  and  $\kappa_q$  in (6) are modeled through Gaussian and normal inverse Gaussian (NIG) distributions for high and low values of autocorrelation

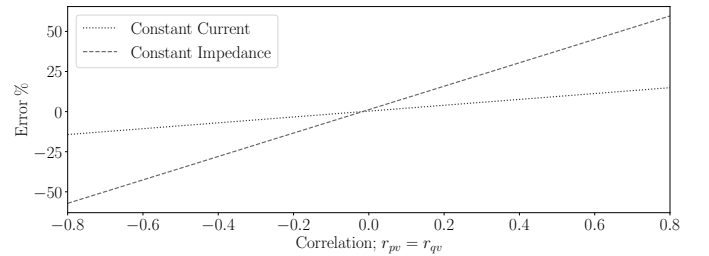


Fig. 2: Percent error on covariances, calculated with (22) using  $C_p[\cdot]$  as base.

coefficient. The details to setup Gaussian and NIG distributions can be found in [21]. The case study simulates three scenarios as follows:

- S0: simulates constant power loads, i.e.,  $\gamma = 0$ .
- S1: simulates constant current loads, i.e.,  $\gamma = 1$ .
- S2: simulates constant impedance loads, i.e.,  $\gamma = 2$ .

The processes  $\kappa_p$  and  $\kappa_q$  are simulated with the following statistical properties:  $\sigma_p = 0.0117$  pu and  $\sigma_q = 0.01435$  pu for Gaussian distribution; and  $k_p = 100.11$ ,  $\delta_p = 0.0141$ ,  $k_q = 37.70$  and  $\delta_q = 0.00753$  for NIG. Note that these parameters are taken from real-world load measurement data and were reported in [21]. The highest and lowest values of autocorrelation coefficients reported in [21] are as follows:  $\alpha_p = 0.045s^{-1}$  and  $\alpha_q = 0.1115s^{-1}$  for high speed; and  $\alpha_p = 0.0048s^{-1}$  and  $\alpha_q = 0.0041s^{-1}$  for low speed processes.

First, we show that the statistical properties of  $p_L$  and  $q_L$  are modified when the voltage dependence of the loads is altered, i.e.,  $\gamma = 0 \rightarrow 2$ . This is illustrated in Fig. 3, which shows the PDFs of  $\kappa_p$  and  $\kappa_q$  at bus 5 for Gaussian distribution. Since,  $\kappa_p$  and  $\kappa_q$  are not affected by the exponent  $\gamma$  they reach the same distributions at stationarity for the three scenarios.

Figure 4 shows the PDFs of  $p_L$  and  $q_L$  at bus 5. This figure shows that  $p_L$  and  $q_L$ , for different values of  $\gamma$ , reach different PDFs at stationarity. This happens despite the fact that  $\kappa_p$  and  $\kappa_q$  have same PDFs at stationarity. The means of  $p_L$  and  $q_L$  are not affected due to the voltage dependence of the loads. This is in accordance with the discussion in Section IV and follows (16).

The only differences that be observed in Fig. 4 are in the variances of  $p_L$  and  $q_L$ . The differences in variances of  $p_L$  and  $q_L$  for the three scenarios are quantified using the standard deviations of  $p_L$  and  $q_L$  as follows. The percent increment in

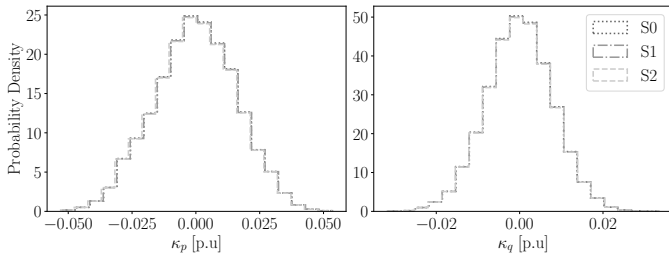


Fig. 3: Probability distribution of  $\kappa_p$  and  $\kappa_q$  modeled via Gaussian distribution at bus 5 for all scenarios.

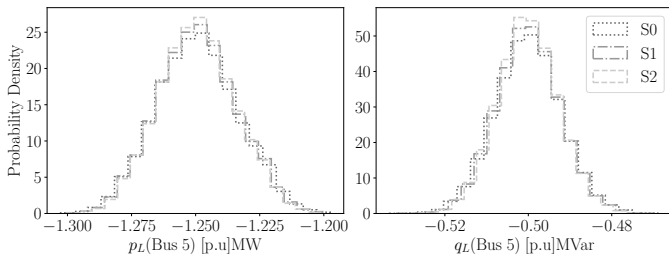


Fig. 4: Probability distribution of  $p_L$  and  $q_L$  at bus 5 modeled via Gaussian distribution for all scenarios.

the standard deviation of  $p_L$  and  $q_L$  from scenario S0 to S2 are  $-7.1\%$  and  $-8.9\%$ , respectively.

Similar differences in the standard deviations of  $p_L$  and  $q_L$  of other load buses, i.e., 6 and 8, are observed. This result is again in conformity with the discussion in Section IV. The fact that the variances of  $p_L$  and  $q_L$  are decreased when the voltage dependence is increased implies that  $v$  has a negative dependence on  $\kappa_p$  and  $\kappa_q$ , and (21) is the proof of this.

The results discussed above imply that, while the mean value of  $v$  is not modified, its variance changes when the voltage dependence of the load changes. This is confirmed by (28) and (29), which indicate that the mean of  $v$  depends on the means of  $p_L$  and  $q_L$ , while the variance of  $v$  depends on the variances and covariances of  $p_L$  and  $q_L$ . To verify this, the variances of  $v$  at bus 5 for all the scenarios are evaluated. The standard deviation of  $v$  for different values of  $\gamma$  are observed to increase from S0 to S1 with  $-11.9\%$  and from S0 to S2 with  $-20.9\%$ .

As  $V[p_L]$  and  $V[q_L]$  are decreased when  $\gamma$  is increased, one might infer that the decrement in  $V[v]$  is solely due to the decrement in  $V[p_L]$  and  $V[q_L]$ . However, from (29), it is obvious that  $V[v]$  also depends on  $C(p_L, q_L)$ . To observe the effect of  $C(p_L, q_L)$  on  $V[v]$ , it is required that  $V[p_L]$  and  $V[q_L]$  remain constant in all the scenarios.

The differences in  $V[p_L]$  and  $V[q_L]$  are easily removed by heuristically adjusting  $V[\kappa_p]$  and  $V[\kappa_q]$  for the three scenarios. The PDFs of  $p_L$  and  $q_L$  achieved after modifying  $V[\kappa_p]$  and  $V[\kappa_q]$  are shown in Figs. 5 and 6. Figures 5 and 6 illustrate the PDFs of  $p_L$  and  $q_L$  for Gaussian and NIG distributions, respectively. In Figs. 5 and 6, it is visible that the PDFs of  $p_L$  and  $q_L$  for all the scenarios are overlapping and  $V[p_L]$  and  $V[q_L]$  remain the same.

Note that  $C(p_L, q_L)$  for all the scenarios depend not only on  $V[p_L]$  and  $V[q_L]$  but also on  $\alpha_p$  and  $\alpha_q$ , see (24), (25) and (26). It is crucial that  $\alpha_p$  and  $\alpha_q$  are kept constant through all the scenarios, so that the effect of  $C(p_L, q_L)$  on  $V[v]$  can be studied solely due to voltage dependence of loads.

Figures 7 and 8 display the autocorrelation functions of  $p_L$  and  $q_L$  for the Gaussian and NIG distributions for the three scenarios, i.e., S0, S1 and S2. Figures 7 and 8 indicate that the autocorrelation functions of  $p_L$  and  $q_L$  remain the same for all the scenarios.

Next, the voltage at load bus 5 is observed for all the scenarios. Figs. 9 and 10 illustrate the PDFs of  $v$  at bus 5 for

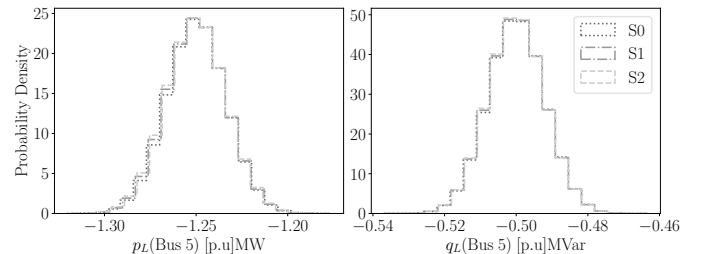


Fig. 5: Probability distribution of active and reactive power modeled using Gaussian distribution at bus 5 for all scenarios.

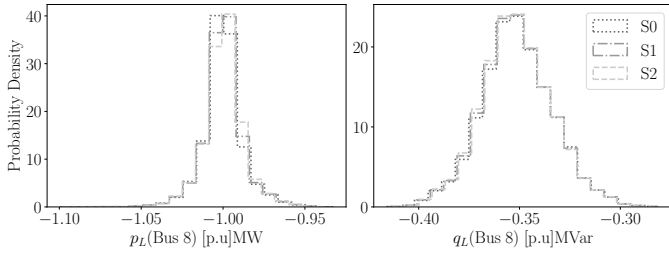


Fig. 6: Probability distribution of active and reactive power modeled using NIG distribution at bus 8 for all scenarios.

the Gaussian and NIG distributions for all the three scenarios. These figures lead to several conclusions, some to be expected and other less intuitive. On the one hand, a reduction in the value of  $\alpha$  causes a shrink in the spread of the PDFs or in other words a reduction in  $V[v]$ . This is consistent with (29) because a modification in  $\alpha$  will modify  $C(p_L, q_L)$ . This has also been reported in other studies, e.g., [19], [20]. On the other hand, modeling  $p_L$  and  $q_L$  with NIG instead of Gaussian distribution causes the PDF of  $v$  to widen and exhibit heavy tails. This result was also reported in [21].

The non-intuitive result that can be inferred from Figs. 9 and 10 is that in the case of both distributions, i.e., Gaussian and NIG, the spread of  $v$  decreases when the voltage dependence of loads is modified from constant power to constant impedance loads, while constant current being in the middle. This is quantified by presenting the values of standard deviations of selected quantities of the WSCC in Tables I to IV.

The results shown in Tables I to IV indicate that the standard deviations of bus voltage magnitudes and reactive power

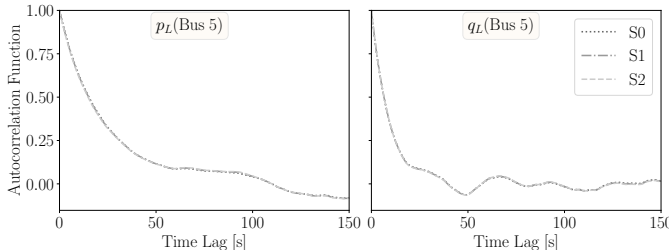


Fig. 7: Autocorrelation function of active and reactive power modeled using Gaussian distribution for highest  $\alpha_p$  and  $\alpha_q$  at bus 5 for all scenarios.

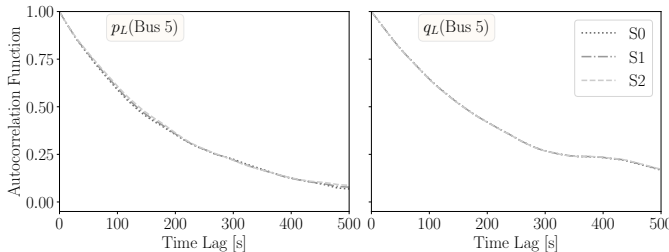


Fig. 8: Autocorrelation function of active and reactive power modeled using NIG distribution for lowest  $\alpha_p$  and  $\alpha_q$  at bus 5 for all scenarios.

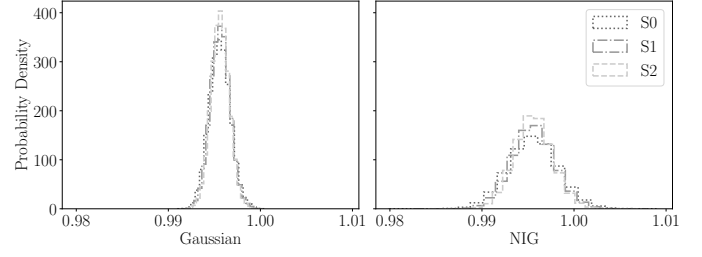


Fig. 9: Probability distribution of voltage magnitude at bus 5 for modeling stochastic processes for highest  $\alpha$  for all scenarios.

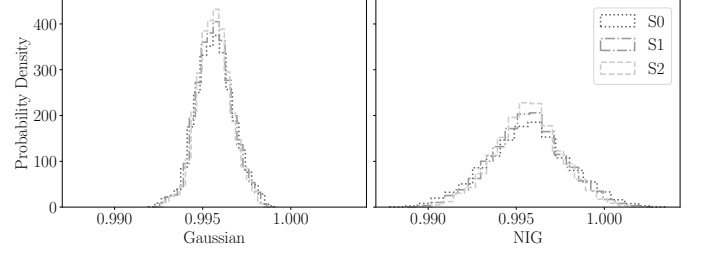


Fig. 10: Probability distribution of voltage magnitude at bus 5 for modeling stochastic processes for lowest  $\alpha$  for all scenarios.

$q_G$  injections of synchronous machines observe significant reduction when the voltage dependence of loads, i.e.,  $\gamma$  is increased from 0 to 2. This reduction in the standard deviation is independent of the statistical properties, i.e., shape and parameters of PDF and autocorrelation of  $p_L$  and  $q_L$ , because they are kept constant in all the scenarios.

The rationale behind the reduction in the standard deviation of  $v$  and consequently of  $q_G$  is easily understandable by carefully inspecting the voltage dependent stochastic load model in (6). From (6), it is obvious that when  $\gamma$  is non-zero, the processes  $\kappa_p$  and  $\kappa_q$  are multiplied either with  $\tilde{v}$  or  $\tilde{v}^2$ . This multiplication introduces a negative correlation between

TABLE I: Standard deviation of power system quantities of WSCC for the three scenarios simulating stochastic loads with Gaussian distribution and highest value of autocorrelation coefficient.

Variable	S0	S1	% inc	S2	% inc
$v(\text{Bus } 5)$	0.001128	0.001035	-8.24	0.000966	-14.36
$v(\text{Bus } 6)$	0.000855	0.000772	-9.71	0.000709	-17.08
$v(\text{Bus } 8)$	0.000845	0.000753	-10.89	0.000684	-19.05
$q_g(\text{G}1)$	0.008409	0.007681	-8.66	0.00711	-15.45
$q_g(\text{G}2)$	0.004262	0.003919	-8.05	0.00366	-14.12
$q_g(\text{G}3)$	0.002816	0.002637	-6.36	0.002513	-10.76

TABLE II: Standard deviation of power system quantities of WSCC for the three scenarios simulating stochastic loads with Gaussian distribution and lowest value of autocorrelation coefficient.

Variable	S0	S1	% inc	S2	% inc
$v(\text{Bus } 5)$	0.001054	0.000978	-7.21	0.000918	-12.9
$v(\text{Bus } 6)$	0.00074	0.000678	-8.38	0.000629	-15
$v(\text{Bus } 8)$	0.000681	0.000619	-9.1	0.000569	-16.45
$q_g(\text{G}1)$	0.008191	0.007501	-8.42	0.006954	-15.1
$q_g(\text{G}2)$	0.00429	0.003944	-8.07	0.003678	-14.27
$q_g(\text{G}3)$	0.002791	0.002633	-5.66	0.002524	-9.57

TABLE III: Standard deviation of power system quantities of WSCC for the three scenarios simulating stochastic loads with NIG distribution and highest value of autocorrelation coefficient.

Variable	S0	S1	% inc	S2	% inc
$v(\text{Bus } 5)$	0.00273	0.00237	-13.38	0.00210	-23.23
$v(\text{Bus } 6)$	0.00268	0.00239	-10.82	0.00218	-18.59
$v(\text{Bus } 8)$	0.00268	0.00236	-11.80	0.00214	-20.08
$q_g(\text{G1})$	0.02137	0.01887	-11.68	0.01697	-20.55
$q_g(\text{G2})$	0.01304	0.01197	-8.22	0.01117	-14.33
$q_g(\text{G3})$	0.01068	0.01003	-6.15	0.00955	-10.64

TABLE IV: Standard deviation of power system quantities of WSCC for the three scenarios simulating stochastic loads with NIG distribution and lowest value of autocorrelation coefficient.

Variable	S0	S1	% inc	S2	% inc
$v(\text{Bus } 5)$	0.002307	0.002049	-11.21	0.001844	-20.07
$v(\text{Bus } 6)$	0.002338	0.002149	-8.07	0.002002	-14.37
$v(\text{Bus } 8)$	0.001909	0.001735	-9.14	0.001603	-16.05
$q_g(\text{G1})$	0.020329	0.018151	-10.72	0.016439	-19.14
$q_g(\text{G2})$	0.012761	0.011720	-8.16	0.010922	-14.41
$q_g(\text{G3})$	0.011095	0.010523	-5.15	0.010091	-9.04

the final load consumption processes, i.e.,  $p_L$  and  $q_L$ . Refer to Section IV for a detailed discussion.

References [6] and [7] indicate that a positive correlation between  $p_L$  and  $q_L$ , when the load is not voltage dependent, results in an increase in the standard deviation of the bus voltage magnitudes and other power system quantities. On the other hand, in this study a decrease in the standard deviation of power system quantities is observed. This decrease is a consequence of the introduction of negative correlation among  $p_L$  and  $q_L$ , which causes the actual correlation to decrease when  $\gamma$  is increased from  $0 \rightarrow 2$ .

For this reason, the active and reactive power load consumption processes at each load bus are considered and the correlation between them is observed by visualizing the scatter plot of  $p_L$  versus  $q_L$ . Figure 11 illustrates the scatter plot of  $p_L$  versus  $q_L$  at bus 5 for NIG distribution at highest autocorrelation simulated for scenarios S0 and S2. The correlation between  $p_L$  versus  $q_L$  at load buses is quantified in Table V. Fig. 11 and Table V show that when  $\gamma$  is increased from 0 to 2, the correlation between  $p_L$  and  $q_L$  is increased in the negative direction, which means that  $p_L$  and  $q_L$  are negatively correlated. This results in the reduction in standard deviation of  $v$  and other quantities. This is consistent with the discussion in Section IV.

## VI. CONCLUSIONS

This paper studies the impact of voltage dependence of the stochastic loads on the correlation of active and reactive power, and consequently on the dynamic of the power system. The paper shows that an increment in the voltage dependence of the loads causes a reduction in the variances and covariances of active and reactive load power consumption. The reduction in the covariances while keeping variances constant causes a

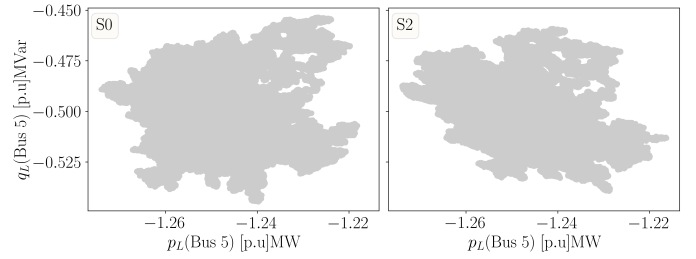


Fig. 11: Scatter plot of active and reactive power modeled using NIG distribution for highest  $\alpha_p$  and  $\alpha_q$  at bus 5 for scenarios S0 and S2.

TABLE V: Standard deviation of power system quantities of WSCC for the three scenarios simulating stochastic loads with NIG distribution and lowest value of autocorrelation coefficient.

Bus	S0	S1	S2
Dist: Gaussian; autocorrelation: high			
5	-0.141	-0.277	-0.389
6	0.133	0.079	0.036
8	0.0565	0.00	-0.033
Dist: NIG; autocorrelation: high			
5	0.036	-0.17	-0.32
6	0.16	0.00	-0.228
8	0.07	-0.07	-0.2
Dist: Gaussian; autocorrelation: low			
5	-0.105	-0.2	-0.3
6	-0.16	-0.237	-0.3
8	0.12	0.07	0.03
Dist: NIG; autocorrelation: low			
5	-0.134	-0.35	-0.49
6	0.062	-0.15	-0.32
8	0.063	-0.066	-0.18

reduction in the variance of the voltages, which compensates the dynamic behavior of the power system.

Simulation results show that increasing the voltage dependence of the stochastic loads causes an improvement in the dynamic behavior of the power system by causing a reduction in the correlation of active and reactive load power consumption. Thus the theoretical developments presented in the paper are fully supported by simulation results.

Future work will consider two directions. One the one hand, extend the analysis of this paper to nonlinear and dynamic load and distributed energy resources models. Then, leverage on the results obtained in this paper to design voltage or frequency regulators able to reduce the effects of the long tails observed in the power system quantities.

## APPENDIX

### A. Stationary Stochastic Process (SSP)

A continuous-time real-valued random process  $X(t)$ ,  $t \in \mathbb{R}$  is considered to be wide-sense stationary if its statistical properties remain invariant with respect to time. This means that the first and second moments, namely the mean and variance, respectively, of  $X(t)$  remain constant with respect to time. Another important characteristic of a stationary stochastic process is that its autocovariance function is not dependent

on time, but rather on the time difference. In other words, the autocovariance function only depends on the time lag between two points in time and is constant throughout the entire process. Mathematically, we can write the properties as:

$$\begin{aligned} E[X(t)] &= E[X(t + \tau)], \\ V[X(t)] &= V[X(t + \tau)], \\ C_X(t_1, t_2) &= E[(X(t_1) - E[X(t)]) \\ &\quad (X(t_2) - E[X(t)])] = C_X(t_1 - t_2). \end{aligned} \quad (31)$$

### B. Voltage as a SSP

The goal of this section is to demonstrate that the voltage  $v$  at the load bus is a stationary stochastic process (SSP) if the load consumption processes, i.e.,  $p$  and  $q$ , are SSPs as well. For this reason, we consider a single load infinite bus system. This system comprises of a bus that can transfer infinite power; a stochastic load that is connected at the load bus; and a line connecting the two buses. The expression for voltage  $v$  at the load bus can be determined as:

$$v = \sqrt{-\left(qx - \frac{v_1^2}{2}\right) \pm \sqrt{\left(qx - \frac{v_1^2}{2}\right)^2 - x^2(p^2 + q^2)}}, \quad (32)$$

where  $v_1$  is the voltage at the infinite bus; and  $x$  is the line impedance.

To show that  $v$  in (32) is a SSP, the properties mentioned in (31) should hold. For this reason, and to simplify the calculations, we linearize (32). A nonlinear expression can be linearized via second-order Taylor Series expansion. Expression for  $v$  in (32) is linearized at the mean values of  $p$  and  $q$ , and written as:

$$v \approx v(p_{L0}, q_{L0}) + \left[ (\Delta p) \frac{\partial}{\partial p} + (\Delta q) \frac{\partial}{\partial q} \right] v(p_{L0}, q_{L0}), \quad (33)$$

where  $\Delta X = X - E[X]$ , this means that  $p$  and  $q$  are centered at zero mean, i.e.,:

$$\Delta X = \int_0^t e^{-\alpha x(t-s)} b_X dW_X, \quad (34)$$

and  $\frac{\partial}{\partial X}$  is the partial derivative with respect to  $X$ .

In (32),  $v$  is a linear combination of two SSPs, i.e.,  $p$  and  $q$ , which are centered at zero-mean. The conditions for the Wold Decomposition Theorem are satisfied. This theorem states that any wide-sense stationary stochastic process can be expressed as the sum of a deterministic component, which is  $v(p_{L0}, q_{L0})$ , and a stationary stochastic component, which is the linear combination of  $\Delta p$  and  $\Delta q$ .

### REFERENCES

[1] C. W. Taylor, *Power System Voltage Stability*. McGraw-Hill, 1994.  
[2] M. K. Pal, "Voltage stability conditions considering load characteristics," *IEEE Trans. on Power Systems*, vol. 7, no. 1, pp. 243–249, Feb. 1992.  
[3] C. A. Cañizares, "On bifurcation voltage collapse and load modeling," *IEEE Trans. on Power Systems*, vol. 10, no. 1, pp. 512–522, Feb. 1995.  
[4] T. Van Cutsem and C. Vournas, *Voltage Stability of Electric Power Systems*. New York, NY: Springer Science, 1998.

[5] C. A. Cañizares *et al.*, "Voltage stability assessment: Concepts, practices and tools – PES-TR9," IEEE/PES Power System Stability Subcommittee, Tech. Rep., Aug. 2002, technical report, available at <http://www.power.uwaterloo.ca>.  
[6] M. Adeen and F. Milano, "Modeling of correlated stochastic processes for the transient stability analysis of power systems," *IEEE Transactions on Power Systems*, vol. 36, no. 5, pp. 4445–4456, 2021.  
[7] G. M. Jónsdóttir and F. Milano, "Modeling correlation of active and reactive power of loads for short-term analysis of power systems," in *IEEE Int. Conf. on Environment and Electrical Eng.*, 2020, pp. 1–6.  
[8] H. Renmu, M. Jin, and D. Hill, "Composite load modeling via measurement approach," *IEEE Transactions on Power Systems*, vol. 21, no. 2, pp. 663–672, 2006.  
[9] S. Son *et al.*, "Improvement of composite load modeling based on parameter sensitivity and dependency analyses," *IEEE Transactions on Power Systems*, vol. 29, no. 1, pp. 242–250, 2014.  
[10] D. Hill, "Nonlinear dynamic load models with recovery for voltage stability studies," *IEEE Transactions on Power Systems*, vol. 8, no. 1, pp. 166–176, 1993.  
[11] D. Karlsson and D. Hill, "Modelling and identification of nonlinear dynamic loads in power systems," *IEEE Transactions on Power Systems*, vol. 9, no. 1, pp. 157–166, 1994.  
[12] W. Xu and Y. Mansour, "Voltage stability analysis using generic dynamic load models," *IEEE Transactions on Power Systems*, vol. 9, no. 1, pp. 479–493, 1994.  
[13] P. Kundur, *Power System Stability and Control*. Mc Graw-Hill, 1994.  
[14] J. V. Milanovic *et al.*, "CIGRE WG C4.605: Modelling and aggregation of loads in flexible power networks," 2014.  
[15] A. Arif, Z. Wang, J. Wang, B. Mather, H. Bashualdo, and D. Zhao, "Load modeling—a review," *IEEE Transactions on Smart Grid*, vol. 9, no. 6, pp. 5986–5999, 2018.  
[16] F. Milano and R. Zárate-Miñano, "A systematic method to model power systems as stochastic differential algebraic equations," *IEEE Trans. on Power Systems*, vol. 28, no. 4, pp. 4537–4544, Nov. 2013.  
[17] K. Wang and M. L. Crow, "Numerical simulation of stochastic differential algebraic equations for power system transient stability with random loads," in *2011 IEEE Power and Energy Society General Meeting*, 2011, pp. 1–8.  
[18] G. M. Jónsdóttir, M. Adeen, R. Zárate-Miñano, and F. Milano, "Modelling power systems with stochastic processes," in *Advances in Power System Modelling, Control and Stability Analysis*. The IET, 2022, pp. 133–174.  
[19] M. Adeen and F. Milano, "On the impact of auto-correlation of stochastic processes on the transient behavior of power systems," *IEEE Transactions on Power Systems*, vol. 36, no. 5, pp. 4832–4835, 2021.  
[20] M. Adeen and F. Milano, "On the dynamic coupling of the autocorrelation of stochastic processes and the standard deviation of the trajectories of power system variables," in *IEEE PES General Meeting*, Washington, DC, 2021.  
[21] M. Adeen and F. Milano, "On the impact of data-driven stochastic load models on power system dynamics," in *2023 IEEE Power Energy Society General Meeting (PESGM)*, 2023.  
[22] B. Øksendal, *Stochastic Differential Equations: An Introduction with Applications*. New York, 6th ed.: Springer, 2003.  
[23] E. Klöden and E. Platen, *Numerical Solution of Stochastic Differential Equations*, 3rd ed. Springer, 1999.  
[24] E. Klöden, E. Platen, and H. Schurz, *Numerical Solution of SDE Through Computer Experiments*. New York, NY, third edition: Springer, 2003.  
[25] A. Ahmed *et al.*, "A novel framework to determine the impact of time varying load models on wind dg planning," *IEEE Access*, vol. 9, pp. 11 342–11 357, 2021.  
[26] M. Adeen and F. Milano, "Stochastic aggregated dynamic model of wind generation with correlated wind speeds," *Electric Power Systems Research*, vol. 212, p. 108312, 2022.  
[27] L. A. Goodman, "On the exact variance of products," *Journal of the American Statistical Association*, vol. 55, no. 292, pp. 708–713, 1960.  
[28] G. W. Bohrnstedt and A. S. Goldberger, "On the exact covariance of products of random variables," *Journal of the American Statistical Association*, vol. 64, no. 328, pp. 1439–1442, 1969.  
[29] F. Milano, "A Python-based software tool for power system analysis," in *IEEE PES General Meeting*, Vancouver, BC, Jul. 2013.